Pergamon

Experimental study of europium (III) coprecipitation with calcite

L. Z. LAKSHTANOV[1,2,*] and S. L. S. STIPP[1]

[1]Geological Institute, Copenhagen University, Øster Voldgade 10, DK-1350 Copenhagen K, Denmark
[2]Institute of Experimental Mineralogy RAS,; 142432 Chernogolovka, Russia

Abstract—Partitioning of Eu(III) in calcite, $CaCO_3$, was evaluated with the aim of collecting data on partition coefficients and to enhance understanding of the incorporation mechanisms. This information will aid in the interpretation of geological processes from rare Earth element (REE) data and in the use of Eu(III) as a chemical analogue for the trivalent actinides, particularly Am(III) and Cm(III). Coprecipitation experiments were carried out by the constant addition method at 25°C and P_{CO_2} = 1 atm. Eu(III) was strongly partitioned from the solution into calcite. For dilute solid solutions (X_{Eu} < 0.001), Eu partition coefficients were estimated to be 770 ± 290 and found to be independent of calcite precipitation rate in the range of 0.02 to 2.7 nmol mg^{-1} min^{-1}. This could be explained by the approximately equal values of the Eu partition and adsorption coefficients. Several solid solution models were tested. A vacancy model for $Eu_2(CO_3)_3$-$CaCO_3$ is consistent with the experimental results and constraints on geometry for Eu fit in the calcite lattice. For low Eu content, vacancy density is independent of Eu concentration in the solid so logarithm of the ion activity product, log $(Eu)^2(CO_3^{2-})^3$, depends linearly on log X_{Eu}^2. The fit of the data to such a model is good evidence that Eu(III) is taken up as a true solid solution, not simply by physical trapping. A model using $EuOHCO_3$-$CaCO_3$ is also consistent with the uptake stoichiometry, but $EuOH^{2+}$ substitution for Ca^{2+} would be expected to distort the calcite structure more than is compatible with such a high K_D. Several other models, including $EuNa(CO_3)_2$-$CaCO_3$, were abandoned because their stoichiometric relationships did not fit the experimental data. *Copyright © 2004 Elsevier Ltd*

1. INTRODUCTION

Prediction of trace component migration in the environment requires detailed understanding of the processes that control the interaction of metal ions with minerals and rocks. Among the controlling processes: surface complexation, ion exchange and coprecipitation, the last is of particular interest because incorporation of a contaminant in a host mineral can lead to its immobilization. Incorporation decreases the possibility of migration more effectively than simple adsorption because incorporated metal has the chance to be remobilized only by a change in chemical conditions that are significant enough to force dissolution of the host mineral (Tesoriero and Pankow, 1996).

Calcite is a common phase in many geological environments, as primary particles in soils and sediments and as coatings or cement between grains and as secondary minerals in fractures and veins. Considerable information about the coprecipitation of divalent metal ions with calcite already exists in the literature, including Sr^{2+} (Lorens, 1981; Mucci and Morse, 1983; Paquette and Reeder, 1995; Parkman et al., 1998), Cd^{2+} (Lorens, 1981; Davis et al., 1987; Tesoriero and Pankow, 1996), Ba^{2+} (Tesoriero and Pankow, 1996), Mn^{2+} (Lorens, 1981; Dromgoole and Walter, 1990); Co^{2+} (Lorens, 1981); Mg^{2+} (Mucci and Morse, 1983); Fe^{2+} (Dromgoole and Walter, 1990); and UO_2^{2+} (Meece and Benninger, 1993). A thorough compilation of coprecipitation data for trace metal uptake by calcite has been made by Rimstidt et al. (1998) and Curti (1999) but data to describe the behavior of the trivalent cations are still mostly lacking.

We chose to investigate the coprecipitation of Eu(III) with calcite, partly to gain a better understanding of REE abundances in sedimentary materials, but mainly because it is a very good chemical analog for the radiologically important Am(III) and Cm(III). The ionic radius of Eu^{3+} (0.95 Å) is not so different from Ca^{2+} (1.00 Å), meaning that if the discrepant charge can be compensated, Eu^{3+} can incorporate into calcite with minimum distortion.

A few experimental studies have been carried out to investigate Eu(III) behavior during its coprecipitation with calcite. Terakado and Masuda (1988) determined the partition coefficients of REE between calcite and aqueous solutions in free-drift experiments. They found that REE concentrations, as well as other solution parameters, changed dramatically with time during precipitation. Using the same free-drift technique, Stipp et al. (2003) studied Eu partitioning between various electrolyte solutions and calcite. The experimental results, as well as field observation (Parekh et al., 1977; Palmer, 1985), prove that calcite has high affinity for Eu(III). Nevertheless, data obtained in this way are difficult to interpret because it is impossible with free-drift data to relate REE concentrations in the solution precisely to the corresponding concentrations in the precipitating calcite. Therefore, applicability of these experimental data is severely limited. Zhong and Mucci (1995) studied coprecipitation with calcite from artificial seawater solutions containing a whole series of REEs. They performed experiments under steady-state conditions using the constant addition technique. This method is probably best because it allows the synthesis of solids with a nearly constant composition at a given precipitation rate. Zhong and Mucci (1995) determined that the partition coefficients of REEs ranged from 4180 for La^{3+} to 60 for Yb^{3+}. For Eu^{3+}, the partition coefficient was determined to average ~ 800, ranging from 210 to 1390.

* Author to whom correspondence should be addressed (leonidl@geo.geol.ku.dk).

Some of the questions arising from the experiments on calcite coprecipitation with trivalent metals, and in particular the REEs, focus on the site and the character of their uptake. Are REEs incorporated directly into the atomic structure of calcite? If so, what is the mechanism for charge compensation where heterovalent substitution results in trivalent ion incorporation in divalent sites?

Piriou et al. (1997) showed, using time-resolved laser fluorescence spectroscopy (TRLFS), that sorbed Eu(III) can substitute for Ca in calcite. Stumpf and Fanghänel (2002) found with the same technique, that Cm(III) is taken up onto bulk calcite by replacement of Ca^{2+} and that the Cm^{3+} ion is coordinated by six oxygens, just as Ca^{2+} is coordinated by six carbonate O's in the calcite structure. There is evidence that Cm^{3+} has no direct contact with water molecules from the aqueous solution. Zhong and Mucci (1995) observed that the Na partition coefficient depends linearly on the total REE content in calcite so on this basis, they suggested that Na^+ may serve to satisfy the excess charge created by substitution of REE^{3+} in Ca^{2+} sites. Elzinga et al. (2002) used extended X-ray absorption fine-structure spectroscopy (EXAFS) to characterize the local coordination of some REEs coprecipitated with calcite. Their results also confirm substitution in the Ca site, but for Nd^{3+} and Sm^{3+}, they suggested sevenfold coordination in a modified Ca site. This contrasted with evidence for Dy^{3+} and Yb^{3+}, which suggested strictly sixfold coordination. Elzinga et al. (2002) concluded, that because Am^{3+} and Cm^{3+} have ionic radii similar to Nd^{3+}, their incorporation into calcite may result in some distortion of the local structure. This prediction was not confirmed by the observations of Stumpf and Fanghänel (2002), whose data showed sixfold coordination of Cm^{3+} incorporated into calcite. Thus, the charge compensation mechanism for such a heterovalent substitution remains unresolved.

Another important question in the understanding of coprecipitation behavior of trivalent cations, is to what extent precipitation rate affects trace component partitioning between a growing solid and the aqueous solution. Because many natural processes occur under chemical conditions that are far from equilibrium, the successful application of experimentally obtained partition coefficients requires knowledge of the significance of precipitation rates.

Many efforts have been made experimentally to study the effect of precipitation rate on partition coefficients of divalent metals (Lorens, 1981; Mucci and Morse, 1983; Tesoriero and Pankow, 1996). Generally, it was found that, the lower the precipitation rate of the host mineral, the closer is the tracer's partition coefficient to its equilibrium value. Thus, increasing precipitation rate enriches the host mineral with the tracer if its equilibrium partition coefficient, $K_D^0 < 1$, and depletes the host when $K_D^0 > 1$. The only experimental work that investigated the influence of calcite precipitation rate on the partition coefficients of trivalent metals (REEs) is that by Zhong and Mucci (1995). Their finding, that the partition coefficients of individual REEs are not affected by the calcite precipitation rate, was quite unexpected. Wang and Xu (2001) proposed a conceptual model that takes into account the effect of adsorption on metal partitioning and as a limiting step, assumes the incorporation of adsorbed cations into the bulk calcite structure. This model provides a reasonable, qualitative explanation for the precipi-

tation rate independence of trivalent metal partitioning observed by Zhong and Mucci (1995).

The objective of the work reported here was to investigate calcite's affinity for Eu(III) as a model for the trivalent actinides and to study the partitioning of Eu into calcite precipitated from electrolyte solutions under strictly controlled experimental conditions. Experimental conditions and solution variables, including calcite precipitation rate, pH, P_{CO_2}, and concentrations of Ca and Eu were held constant throughout any given precipitation experiment. By systematically varying Eu concentration and calcite precipitation rate, their influence on Eu partitioning could be determined. Using the stoichiometric relationships of the data for Eu/Ca substitution and the thermodynamic theory of solid solution formation (Lippmann, 1980), an effort has been made to elucidate the mechanism of Eu incorporation into calcite.

1.1. Partition Coefficient

As a solid grows from a solution at equilibrium, trace components distribute between the two phases in a characteristic manner. A general form of the fundamental law that controls this distribution was introduced by Henderson and Kracek in 1927. For a particular case of divalent metal partitioning between calcite and aqueous solution, the partition coefficient can be defined as:

$$K_D = \frac{X_{Me}}{X_{Ca}} \frac{[Ca]}{[Me]} \quad (1)$$

where X_{Me} and X_{Ca} represent the molar fractions in calcite and $[Me]$ and $[Ca]$, the molal concentrations in the solution. For conditions where $K_D > 1$, the crystal growing from the solution is enriched in the trace component with respect to the solution; for values where $K_D < 1$, the crystal is depleted in trace component with respect to the solution.

A partition coefficient is assumed to be a function of temperature and pressure, but not of the concentration of the trace metal. Generally, it is possible to obtain K_D from thermodynamic considerations (Rimstidt et al., 1998; Curti, 1999):

$$K_D = \frac{K^s_{Ca}}{K^s_{Me}} \frac{f_{Ca}}{f_{Me}} \frac{\gamma_{Me^{2+}}}{\gamma_{Ca^{2+}}} \quad (2)$$

where K^S_{Ca} and K^S_{Me} represent the solubility products of calcite and the trace metal carbonate, respectively, f_{Ca} and f_{Me} denote the activity coefficients of calcite and the trace metal carbonate, and $\gamma_{Ca^{2+}}$ and $\gamma_{Me^{2+}}$ are the molal scale activity coefficients of Ca^{2+} and Me^{2+} in the aqueous solution.

When both aqueous and solid solutions are ideal, partition coefficients are simply determined by the ratio of the solubility products of calcite and trace metal carbonate:

$$K_D = \frac{K^s_{Ca}}{K^s_{Me}} \quad (3)$$

The above formulation is true as long as the simple substitution of Ca in the calcite lattice by a divalent trace metal, Me^{2+}, is considered. To obtain K_D from thermodynamic considerations for heterovalent substitution, e.g., for substitution of Eu^{3+} for Ca^{2+}, one needs to know the mechanism of Eu incorporation into calcite, which supposes a knowledge of the stoichiometry

of the Eu-Ca substitution reaction. The main problem with that, is knowing the charge compensation mechanism. We plan to show that this stoichiometry can be different depending on the kind of solid solution formed, that is, on the kind of Eu carbonate end-member that results, as well as on the Eu concentration in the solid solution. Therefore, until the stoichiometry of the substitution is elucidated, the a priori use of the common partition coefficient for Eu-Ca substitution makes a little sense. Thus, a partition coefficient as expressed by Eqn. 1 is not necessarily a thermodynamic constant that is independent of Eu concentration and it may reflect only whether precipitated calcite is enriched or depleted by europium with respect to the solution. Moreover, it is well known (Chernov, 1980; Lorens, 1981; Mucci and Morse, 1983; Watson and Liang, 1995; Tesoriero and Pankow, 1996; Wang and Xu, 2001) that when the host mineral precipitates from an aqueous solution, there exist several processes with a time-dependent nature, such as diffusion relaxation in the bulk solid as well as in the contacting solution, that can divert the partition coefficient from its equilibrium value.

2. MATERIALS AND METHODS

For coprecipitation experiments, we used two types of calcite powder. One of them was natural calcite (Mexico) which was crushed and size-separated to remove particles smaller than 1 μm diameter by settling in a water column. The second was reagent grade calcite supplied by Sigma, which had particle size on the order of 10 microns. Surface area of both materials was about the same, 0.25 m^2/g, but the particles of Sigma calcite were much more uniform in size than those of the natural material. Based on sedimentation rates and Scanning Electron (SEM) and Atomic Force (AFM) Microscopy images, diameter of the Sigma powder was determined to be ~10 to 20 μm and that of the natural calcite ranged from ~2 to 100 μm. The exact size distribution of the natural material is not known. The commercial powder was treated to remove the organic inhibitors added during commercial synthesis by recrystallizing several times in vessels of freshly deionized, hot (65°C) water under (100%) CO_2 atmosphere by a method adopted from Stipp and Hochella (1991). The crushed sample was recrystallized in the same way for consistency and also in an attempt to remove the defects introduced by crushing.

A method for the coprecipitation of Eu-bearing calcite was developed for these experiments that was very similar to that described by Tesoriero and Pankow (1996) because it allows not only the synthesis of solids of a nearly constant composition at a given precipitation rate, but also because it allows direct comparison of measured Eu concentration in the solution to its corresponding concentration in a freshly precipitated calcite. For Eu, this was important because of the strong tendency of this ion to distribute into calcite.

For each experiment, usually 100 mL of $NaClO_4$ solution was maintained at 25°C and P_{CO_2} = 1 atm in a jacketed reaction vessel. Weighed amounts of calcite powder were placed into the reaction vessel to equilibrate the solution with calcite and to provide seed material for the precipitation. The powder was maintained in suspension by an overhead propeller stirrer to prevent grinding of the powder against the bottom. To minimize evaporation in long term experiments, the CO_2 gas was first bubbled through a 0.1 mol/L $NaClO_4$ solution before it was bubbled into the reaction vessel.

Precipitation was induced by pumping the two separate solutions, ($Ca(ClO_4)_2$ and Na_2CO_3), into the reaction vessel with a peristaltic pump. The mixing of the two solutions caused calcite precipitation and the rate of solution addition was used as the precipitation rate. Simultaneously, precipitation rate increased until it equaled the addition rate of Ca and carbonate by the peristaltic pump. After steady-state precipitation rate was reached, where solution composition in the reaction vessel (including pH) remained essentially constant, a small aliquot (0.1–1 mL) of 7.5e-3 mol/L $Eu(NO_3)_3$ stock solution (pH ~ 5.1) was added to the initial $Ca(ClO_4)_2$ stock solution. Introduction of the Eu

solution had no measurable effect on carbonate alkalinity or pH. Pumping of the solutions continued as before, at the same rate, until a second steady-state condition was reached where Eu concentration remained constant. In some experiments, a Eu aliquot was added to the initial $Ca(ClO_4)_2$ solution from the beginning and the steady-state condition of constant Eu concentration, was awaited. The aqueous phase was periodically sampled, filtered through 0.2 micron Sartorius filters, and analyzed for Ca and Eu. This second steady-state condition is the most important point in the experiment because the Eu molar fraction in the solid at this second steady-state can be assumed to equal the Eu molar fraction in the initial solution. More correctly, Eu molar fraction in the last precipitate formed at steady state (X_{Eu}) can be expressed as follows:

$$X_{Eu} = \frac{[Eu]^0 - [Eu]^{st}}{[Ca]^0 - [Ca]^{st} + [Eu]^0 - [Eu]^{st}} \qquad (4)$$

where the superscript 0 and the superscript st denote the corresponding molar concentrations in the initial solution and in the reaction vessel at the second steady-state. These values of Eu molar fraction were then used for determination of the Eu partition coefficients and other equilibrium constants corresponding to the various proposed mechanisms for Eu incorporation and the various kinds of Eu-calcite solid solution.

Eu concentrations of the feed solution were chosen such that the solubility products of pure Eu solid phases (such as $Eu_2(CO_3)_3$, $EuOHCO_3$, $Eu(OH)_3$) were by no means exceeded to insure that Eu^{3+} could precipitate as a solid solution and not as a separate, pure Eu phase. Aqueous speciation calculations for all experiments were performed using PHREEQC (Parkhurst and Appelo, 1999) with inclusion in the database of constants for Eu speciation (Hummel et al., 2002).

At the end of each experiment, the solid phase was rinsed for a few minutes with a calcite-saturated solution, dried at 90°C for a day, and then weighed. Several samples with the highest Eu loadings were checked by X-ray diffraction. Calculations with expected intensities for other Eu phases indicate that within a detection limit of ~1%, no crystalline materials other than calcite were found. A part of each solid sample was dissolved in 3.5 mol/L HNO_3 and analyzed for Eu and Na. The solid composition values for Eu were not used for examination of X_{Eu} values obtained using Eqn. 4 because of the large errors in determination of solid composition. They resulted from the errors of the overgrowth mass estimation as well as from the uncertainties of the overgrowth composition over the course of the pre–steady state period. Ca and Na concentrations were determined by atomic absorption spectrophotometry (AAS) (Perkin-Elmer 5100) with precision better than ±2%. Eu concentration was determined by ICP-MS using the isotope dilution method (Baker et al., 2002) on a portion of the solution spiked with Eu and passed through a resin column to reduce interference by Ca^{2+}. The detection limit for Eu was ~ 0.05 nmol with precision ±2% for solutions with [Eu] > 1 nmol and ±5% for solutions where [Eu] < 1 nmol.

3. RESULTS AND DISCUSSION

A first steady-state condition with constant calcite precipitation rate was usually reached within 25–30 h after beginning a run, depending on initial $Ca(ClO_4)_2$ concentration. After the aliquot of Eu stock solution was added, Eu concentration in the reaction solution increased and a second steady-state condition with constant Eu concentration was attained within 3–5 d, depending on Ca and Eu initial concentrations. As Tesoriero and Pankow (1996) reported for Cd coprecipitation with calcite, attainment of the second steady-state condition is direct evidence of solid solution formation. During such experiments, the increase in available surface area is insignificant, certainly incompatible with the increased rates of Eu removal. If simple adsorption was responsible for uptake, rather than reaching steady-state, Eu concentration would continue to increase in the reaction vessel until the $Eu_2(CO_3)_3$ or $EuOHCO_3$ solubility product was reached and a separate, pure phase would precipitate.

Table 1. Experimental conditions for coprecipitation runs.

N^a	$[Ca]^0$ (mol/L)	$[Ca]$ (mol/L)	$[Eu]^0$ (mol/L)	$[Eu]$ (mol/L)	Ionic strength (mol/L)	pH	Run duration[b] (min)	R (10^{-9} mol/mg min)	X_{Eu}^c	X_{Eu}^d	X_{Na}^d	K_D^e
1n	0.0284	0.0109	2.76e-7	1.85e-10	0.1327	6.16	4350	0.15	1.58e-5	—	—	929
2n	0.0203	0.0078	1.04e-7	1.36e-10	0.0381	6.11	4560	0.09	2.21e-5	—	—	477
3n	0.0340	0.0101	1.61e-6	4.30e-10	0.1103	6.06	3960	0.11	6.71e-5	—	8.7e-4	1575
4n	0.0342	0.0100	1.58e-7	1.10e-10	0.1100	6.07	6480	0.08	6.58e-6	—	7.0e-4	588
5n	0.0341	0.0101	1.92e-6	5.47e-10	0.0803	6.09	5880	0.09	8.09e-5	—	4.8e-4	1492
6n	0.0350	0.0108	1.23e-6	9.30e-10	0.0824	6.08	5940	0.17	5.17e-5	—	1.35e-3	601
7n	0.0347	0.0094	2.90e-7	1.51e-10	0.0960	6.07	5550	0.12	1.17e-5	—	—	729
8s	0.0643	0.0120	1.21e-6	5.32e-10	0.0960	6.14	5130	1.36	2.29e-5	2.1e-5	2.1e-4	518
9s	0.0645	0.0122	1.12e-6	4.05e-10	0.0968	6.09	4350	2.71	2.29e-5	2.1e-5	2.4e-4	694
10n	0.0370	0.0113	1.51e-6	6.58e-10	0.0830	6.02	6300	0.02	5.86e-5	—	—	1006
11n	0.0336	0.0084	3.00e-6	1.51e-9	0.0667	6.07	4020	0.20	1.19e-4	—	—	658
12s	0.0374	0.0119	1.50e-5	6.67e-9	0.0854	6.02	5760	0.20	5.89e-4	—	—	1052
13s	0.0622	0.0110	1.29e-6	4.27e-10	0.0812	6.03	5580	0.67	2.52e-5	1.6e-5	3.7e-4	650
14s	0.0605	0.0098	3.27e-6	8.36e-10	0.0854	6.05	4440	0.66	6.45e-5	2.3e-5	—	752
15s	0.0637	0.0128	8.0e-6	2.88e-9	0.0798	6.02	6360	0.55	1.57e-4	1.1e-5	—	698
16s	0.0613	0.0103	4.02e-6	1.30e-9	0.0848	6.04	4800	0.61	7.84e-5	7.2e-5	2.7e-4	618
17s	0.0627	0.0123	1.50e-5	4.82e-9	0.0610	6.01	7080	0.52	2.98e-4	1.3e-5	1.0e-4	756
18s	0.0375	0.0110	1.98e-6	1.42e-9	0.0584	6.01	6300	0.04	7.49e-4	—	—	580
19s	0.0362	0.0098	1.01e-5	4.70e-9	0.0601	6.05	6300	0.10	3.79e-4	—	—	790
20s	0.0368	0.0107	1.01e-5	6.93e-9	0.0584	6.03	6990	0.04	3.83e-4	—	—	590
21s	0.1163	0.0127	7.51e-6	1.09e-9	0.1481	6.05	6210	1.61	7.24e-5	6.7e-5	—	844
22s	0.1165	0.0143	1.51e-5	2.80e-9	0.1629	6.08	6210	1.60	1.48e-4	1.1e-4	—	756
23s	0.1168	0.0126	2.98e-6	2.95e-10	0.1578	6.03	5640	1.40	2.86e-5	3.0e-5	—	1222
24s	0.1176	0.0126	8.30e-7	3.25e-10	0.1428	6.03	5880	1.41	7.89e-6	7e-6	—	306

[a] n and s indicate runs with natural and synthetic calcite, respectively.
[b] Time from the moment of Eu addition to the end of the run.
[c] Calculated from the solution concentration data according to Eqn. 4.
[d] Obtained from the solid concentration data.
[e] Calculated according to Eqn. 1.

The experimental conditions, including aqueous and solid compositions as well as calcite precipitation rate, are given in Table 1. One can see that Eu molar fractions calculated using Eu and Ca aqueous concentrations in the feed solution are always higher than those obtained using their concentrations in the calcite overgrowths. This occurs because composition of the solid is not uniform. Aside from the mass of the calcite seed grains, with their overgrowths precipitated during the attainment of first steady-state (which are free of Eu and easy to account for), the total mass of the resulting material also contains overgrowths with Eu coprecipitated during the period where the system was attempting to reach its second steady-state condition. From the moment when Eu was first added to the $Ca(ClO_4)_2$ feed solution until the attainment of the second steady-state condition, Eu concentration in the solution was not constant, so its incorporation into calcite was not constant. Therefore, for the calculation of Eu partition coefficients, we used the values of Eu molar fraction in calcite calculated from the solution concentration data only. In some runs, where precipitation rates were low, the overgrowth mass was too small to allow determination of Eu or Na with sufficient accuracy to be useful. Thus the data determined from the solids have not been used for any of the calculations.

3.1. Precipitation Rate Effect

To obtain the equilibrium K_D values required for modeling, the system is assumed to be in equilibrium, that is, the chemical potential of each component is the same everywhere in the system. This assumes that all phases are equilibrated with each other and the spatial distribution of a component is uniform. Partition coefficients determined for natural systems as well as those estimated from experimental data usually differ from equilibrium values because the conditions both in natural environments and in experiments rarely reach equilibrium. Thus, distribution of a trace component in the growing crystal is effectively determined by some kinetic process. It is well-known that the trace concentration is controlled by the mechanisms of statistical selection in the interfacial region and diffuse relaxation in the bulk crystal and in the surrounding solution. The composition of the adsorption layer is generally different from that in the bulk crystal. If the crystal grows, some ions bound in the surface layer have to be transferred back to the solution. But if crystal growth is rapid, they may be trapped and buried in the freshly precipitated material, resulting in solid concentrations that deviate substantially from those predicted by equilibrium partitioning between the crystal and its surroundings. The effectiveness of this entrapment process depends on the interplay between the growth rate of the crystal and the diffusivity in the boundary layer of the crystal, which determines how efficiently a component can reach the surface by diffusion through the solution. Models developed to explain the partitioning of trace elements between a solution and a growing crystal are based on the Berthelot-Nernst distribution law (McIntire, 1963):

$$k_D = \frac{C_s}{C_l} \quad (5)$$

where k_D is the distribution coefficient, C_s and C_l are concentrations of the trace component in the solid and the liquid. Diffuse relaxation of the distribution coefficient depends on precipitation rate as follows (Chernov, 1980):

$$k_D = k_D^0 + (k_{st} - k_D^0)\exp\left(-\frac{D_s}{R \cdot h}\right) \quad (6)$$

where k^0_D represents the equilibrium distribution coefficient, k_{st}, the distribution coefficient on the growing step of the crystal, D_s, the diffusion coefficient of trace component in the crystal, R, the linear normal growth rate and h, the height of the growing step.

This equation does not take into consideration the similar diffuse relaxation in the surrounding solution where interplay between the crystal growth rate, the transfer of a species from the solution to the surface, and chemical reaction at the surface take place. During fast crystal growth, the rate of the adsorption process is often diffusion controlled and the concentration depends on the distance from the crystal surface. Therefore, at high precipitation rates, a growing crystal may trap a species at the ratio of their diffusivities in the bulk solution, which is always nearly 1, and k_D tends to 1. When diffusion is not limiting, the solution is able to supply the boundary layer, adsorption is nearly at equilibrium, so at very low precipitation rates, k_D approaches its equilibrium value. Between these limiting cases, a variety of opportunities for k_D exist to take values from k_D to 1. Depending on the ratio between the equilibrium adsorption and distribution coefficients, k_{st}^0 and k_D^0, k_D may even be an extreme function of the precipitation rate (Dubinina and Lakshtanov, 1997). On the other hand, at low to moderate precipitation rates and when the local conditions within the boundary (or adsorption) layer approach equilibrium, Eqn. 6 can be considered as a good approximation. It can be easily seen from this equation that a special case exists when kst^0 and kD^0 have similar values. Then, the distribution coefficient, k_D, is independent of precipitation rate and there is a proximity between k_D and kD^0 for any value of precipitation rate. This is very similar to the concept of Wang and Xu (2001).

For highly charged cations such as Eu, the distribution coefficient is independent of precipitation rate because their adsorption coefficients are large (Zhong and Mucci, 1995) and close to the value of the partition coefficient. Figure 1 shows the Eu partition coefficient, as expressed by Eqn. 1, plotted as a function of calcite precipitation rate. There is essentially no dependence of the Eu partition coefficient on precipitation rate over the range from 0.02 to 2.7 nmol mg^{-1} min^{-1}. Moreover, there is no difference in behavior for the two calcite powders, in spite of the difference in their size distribution functions.

For a spherical particle, Chernov (1980) expressed the linear growth rate, v, as:

$$v = \frac{\omega\beta(\Delta C)}{1 + \dfrac{\beta r}{D_l}} \quad (7)$$

where β represents the kinetic coefficient of crystal interface growth, ω denotes the molecular volume, ΔC, the oversatura-
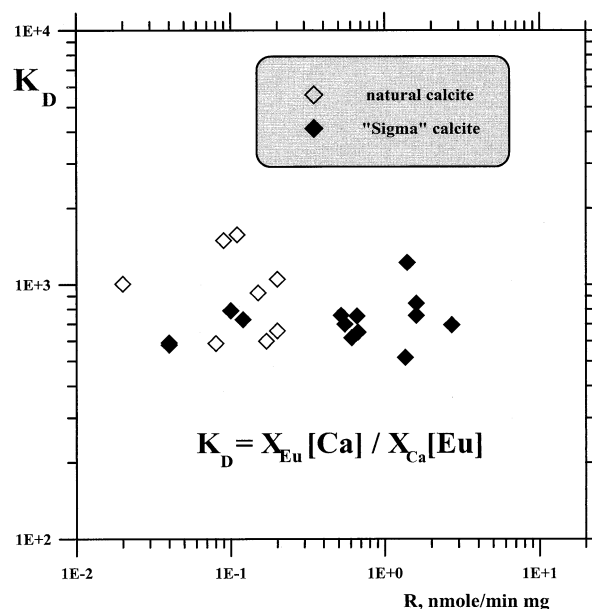

Fig. 1. Eu partition coefficient, K_D, plotted as a function of calcite precipitation rate, R. Open symbols denote K_D obtained for crushed and sieved natural calcite; closed symbols, commercial, synthetic "Sigma" calcite.

tion value, D_l, diffusion coefficient in the solution and r, the radius of the particle. Although the two sample materials have nearly the same specific surface area, the crushed natural calcite consists of particles with a much wider size distribution. At the same supersaturation value, small particles ($\sim$1 μm) must grow noticeably faster than larger particles (10–100 μm). For example, depending on temperature, the growth rates of small (a few microns) and larger (tens and hundreds of microns) particles of quartz can differ by several times (Dubinina and Lakshtanov, 1997). Therefore, if Eu partitioning to calcite is to be affected by calcite precipitation rate, there should be a distinct difference between the two powders but Figure 1 shows there is no significant difference in the partition coefficients for the two materials. This is also consistent with an independence of Eu partitioning on precipitation rate. Thus, one can suppose that all partition coefficients obtained at the various precipitation rates are free of kinetic effects and can be considered as equilibrium values.

Figure 2 shows a plot of the Eu molar fraction in the solid, X_{Eu}, vs. the steady-state ratio of Eu and Ca concentrations in the solution, [Eu]/[Ca], which is probably very close to the equilibrium case. The relationship is linear as well as nearly directly proportional (slope = 1). Such dependence is a reason why the Eu partition coefficient, K_D, is independent of both X_{Eu} and [Eu] (not shown here), although in the case of heterovalent substitution, when several mechanisms of tracer incorporation can exist, K_D as expressed by Eqn. 1 is a relatively abstract quantity. The average value determined for the Eu partition coefficient, 770, is very close to 800, the average obtained by Zhong and Mucci (1995). However, they reported that the partition coefficients of the LREEs, including Eu, showed a positive correlation with their absolute solution concentrations, so an increase of [Eu] has to be associated with a
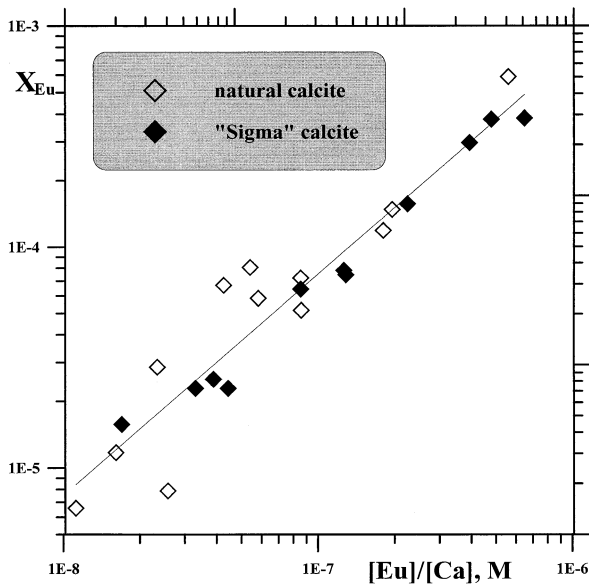
Fig. 2. Eu molar fraction in the solid, X_{Eu}, as a function of the steady state Eu to Ca concentrations ratio in the solution, [Eu]/[Ca]. The straight line is an approximation equation, $X_{Eu} = 769*([Eu]/[Ca])^{1.001}$. Open symbols denote results obtained for the natural calcite; closed symbols, the commercial powder, "Sigma" calcite.

disproportional decrease of X_{LREE}, not an increase as Zhong and Mucci (1995) write. This means that in the case of europium, $X_{Eu} \sim [Eu]^n$ with $n > 1$. We show, in the following discussion, that would be impossible to explain using any of the conceivable models of Eu incorporation into calcite.

3.2. Modes of Eu Partitioning to Calcite

Let us use the relationship between mole fraction in the solid and relative solution concentration to consider several solid solution models for explaining charge compensation for Eu coprecipitation in calcite.

3.2.1. $Eu_{2x}(CO_3)_3$-$CaCO_3$ Solid Solution

Consider the $Eu_{2x}(CO_3)_3$-$CaCO_3$ solid solution where x symbolizes a cation vacancy. A crystal usually contains many types of defects. One category can be distinguished as an "outer" defect, where an admixed or trace atom is included together with a vacancy to compensate for the charge discrepancy between the trace and the substituted atom. In addition, a real crystal contains many of its own or "intrinsic" defects that are not immediately related to the presence of trace atoms (Urusov et al., 1997; Urusov and Dudnikova, 1998). Long ago, Kelting and Witt (1949) developed a thermodynamic description of the interaction of a heterovalent tracer with vacancies using as an example, the halogenides of divalent alkali metals. Adopting that method, we can describe incorporation of trivalent Eu^{3+} into calcite by formation of a cation vacancy, x, as:

$$2Eu^{3+} + 3Ca_s^{2+} = 2Eu_s^{3+} + x + 3Ca^{2+}. \tag{8}$$
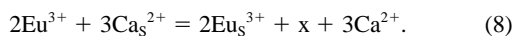
Two limiting cases can be distinguished.

a) For situations where Eu concentration in the solid is much

higher than that of intrinsic defects, then vacancy concentration is determined by Eu concentration in the solid: $X_x = \frac{1}{2} X_{Eu}$.

Thus, substituting for X_x, the equilibrium constant for the substitution model represented by Eqn. 8 can be written as:

$$K_1 = \frac{X_{Eu}^2 X_x}{X_{Ca}^3} \frac{(Ca^{2+})^3}{(Eu^{3+})^2} = \frac{X_{Eu}^3}{X_{Ca}^3} \frac{(Ca^{2+})^3}{(Eu^{3+})^2} \tag{9}$$

where the factor, $\frac{1}{2}$, is included in the constant.

Solubility of the solid solution is described by two equations (Lippmann, 1980), one relating the concentration of $Eu_{2x}(CO_3)_3$ in the ideal solid solution with the activities of the Eu^{3+} and CO_3^{2-} ions in the aqueous solution:

$$(Eu^{3+})^2(CO_3^{2-})^3 = K^s_{Eu_{2x}(CO_3)_3} X_{Eu_{2x}(CO_3)_3} \tag{10}$$

and the other relating the concentration of $CaCO_3$ in the ideal solid solution to the activities of the Ca^{2+} and CO_3^{2-} ions in the solution, i.e.,

$$(Ca^{2+})^3(CO_3^{2-})^3 = K^s_{Ca}{}^3 X_{Ca}{}^3, \tag{11}$$

where $K^S_{Eu_2x(CO_3)_3}$ and K^S_{Ca} represent the solubility products for the $Eu_{2x(CO_3)_3}$ and $CaCO_3$ end members.

Dividing Eqn. 11 by Eqn. 10, we have

$$\frac{X_{Eu_2x(CO_3)_3}}{X_{Ca}^3} \frac{(Ca^{2+})^3}{(Eu^{3+})^2} = \frac{K^s_{Ca}{}^3}{K^s_{Eu_2x(CO_3)_3}} = Const. \tag{12}$$

Comparison of Eqn. 12 with Eqn. 9, shows that from Eqn. 12, $X_{Eu_2x(CO_3)_3}$ should be equal to $X_{Eu}{}^3$ from Eqn. 9. So one can rewrite Eqn. 10 as follows:

$$(Eu^{3+})^2(CO_3^{2-})^3 = K^s_{Eu_2x(CO_3)_3}{}^s X_{Eu}{}^3 \tag{13}$$

Inspection of Eqn. 9 shows that if (Ca^{2+}) is constant, as is approximately the case in our experiments because of constant pH and P_{CO2}, then europium activity in solution, (Eu^{3+}), is expected to be proportional to $X_{Eu}{}^{3/2}$ instead of X_{Eu}, which we observe from the experimental data. As well, this applies for the ion activity product, which according to Eqn. 13 is expected to be proportional to $X_{Eu}{}^3$ instead of the experimental slope 1 (Fig. 2). Thus, this model must be abandoned because it contradicts the experimental results.

b) In the case of very low Eu incorporation, where its concentration is much lower than that of intrinsic defects, the concentration of "outer" defects (i.e., those directly connected with incorporated Eu) is negligible. Concentrations of cation- (x) and anion- (y) vacancies should be equal to each other and connected by the equilibrium condition:

$$K_x = (x)(y) \text{ and } (x) = \sqrt{K_x}. \tag{14}$$

One can see that this condition decreases X_{Eu} by one power in the expression for the equilibrium constant of substitution Eqn. 8 compared to Eqn. 9:

$$K_2' = \frac{K'}{\sqrt{K_x}} = \frac{X_{Eu}^2}{X_{Ca}^3} \frac{(Ca^{2+})^3}{(Eu^{3+})^2} \tag{15}$$

For the ion activity products of the end members, Eqns. 10 and 11 are valid as before but in this case, comparison of Eqns. 12 and 15 shows that from Eqn. 10 $X_{Eu_2x(CO_3)_3}$ should be equal to $X_{Eu}{}^2$ from Eqn. 15. For this case, we rewrite Eqn. 10 as:
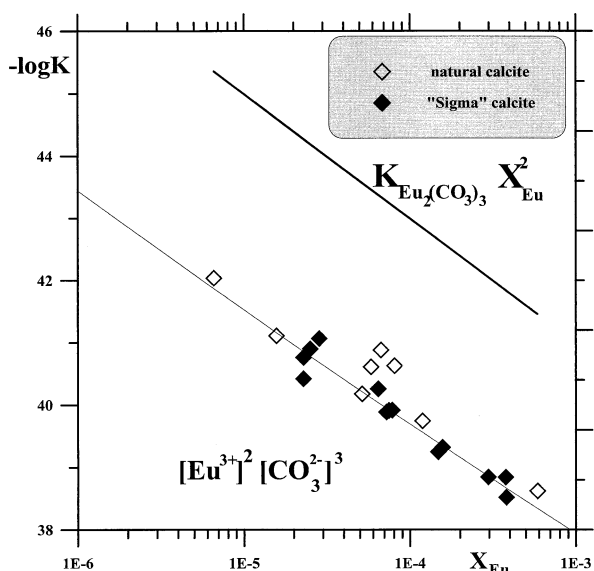
Fig. 3. Ion activity product, $(Eu^{3+})^2 (CO_3^{2-})^3$ vs. Eu molar fraction in the solid, X_{Eu}. The darker line represents the solubility constant for the $Eu_2(CO_3)_3$ end member multiplied by X_{Eu}^2. Open symbols denote results obtained for the natural calcite; closed symbols, "Sigma" calcite.

$$(Eu^{3+})^2(CO_3^{2-})^3 = K^s_{Eu_{2x}(CO_3)_3} X_{Eu}^2 \qquad (16)$$

Thus, in this model, the equilibrium Eu concentration in solution and the ion activity product are both proportional to the europium molar fraction in the solid, X_{Eu}. This relationship corresponds with the experimental data (Figs. 2 and 3).

One can see from Figure 3 that although there are two lines corresponding to each of the sides of Eqn. 16, these lines are essentially parallel; they do not coincide. Extrapolation of the fitting line for the ion activity product's experimental data to $X_{Eu} = 1$ gives the value 33.1 for $-\log K$. In accordance with Eqn. 16, this value is the solubility product of the $Eu_2 x (CO_3)_3$ end-member which must differ from the solubility product of crystalline $Eu_2(CO_3)_3$, $-\log K = 35.0$ (Hummel et al., 2002). Indeed, it has to be expected that the crystal structure for pure $Eu_2(CO_3)_3$ should be different than that of the $Eu_2 x(CO_3)_3$ end-member. When two Eu^{3+} substitute for three Ca^{2+} in the calcite structure; forming the vacancy solid solution, the atomic arrangement of the latter probably to some extent inherits the calcite structure, at least this is true for low Eu content. It is not surprising then, that the solubility of such a disordered $Eu_2 x(CO_3)_3$ is higher than that of $Eu_2(CO_3)_3$.

3.3.2. EuOHCO₃-CaCO₃ Solid Solution

In this case, one can imagine several possibilities depending on the location of hydroxide ion.
a) Simple substitution

$$EuOH^{2+} + Ca_s^{2+} = EuOH_s^{2+} + Ca^{2+} \qquad (17)$$

implies no charge imbalance. Incorporation of the single E_uOH^{2+} unit into the calcite structure implies that OH^- occu-

pies the same site as Eu^{3+}. The equilibrium constant for this substitution is:

$$K_3 = \frac{X_{Eu}}{X_{Ca}} \frac{(Ca^{2+})}{K_{EuOH}(Eu^{3+})(OH^-)} \qquad (18)$$

or

$$K_3' = \frac{X_{Eu}}{X_{Ca}} \frac{(Ca^{2+})}{(Eu^{3+})(OH^-)} \qquad (19)$$

where K_{EuOH} is the formation constant for the $EuOH^{2+}$ aqua complex. The corresponding ion activity product can be written for this case as follows:

$$(Eu^{3+})(OH^-)(CO_3^{2-}) = \frac{K^s_{EuOHCO_3}}{K_{EuOH}} X_{EuOHCO_3}, \qquad (20)$$

where $K^S_{EuOHCO_3}$ represents the solubility product of the EuO-HCO₃ end member. Using the same procedure as in the previous case, one can deduce that (Eqn. 20) equals X_{Eu} from Eqn. 19.

We can see that (Eu^{3+}) is proportional to X_{Eu} and therefore, this model would satisfy the experimental data (Fig. 2). However, substitution of a large entity such as $EuOH^{2+}$ into a Ca site would be expected to lead to a significant distortion of the calcite lattice, resulting in very low partition coefficients, which is at variance with the experimental data. Stumpf and Fanghänel (2002) reported that TRFLS data from Cm(III) incorporated in the same natural calcite that we used, indicated no OH in the first coordination sphere but their recent investigations of Eu(III) in a natural calcite sample, suggest that OH or H_2O may occur in the first coordination shell for Eu(III). Further work on this question is in progress.

b) Another possibility for hydroxide ion is substitution in CO_3^{2-} sites that are separated from sites occupied by Eu^{3+}. This model does not require much distortion of the calcite structure. It implies again, as in case 1, formation of solid solution with vacancies:

$$Eu^{3+} + OH^- + 2Ca_s^{2+} + 2CO_{3s}^{2-} = Eu_s^{3+} + x + OH_s^-$$
$$+ CO_{3s}^{2-} + 2Ca^{2+} + CO_3^{2-} \qquad (21)$$
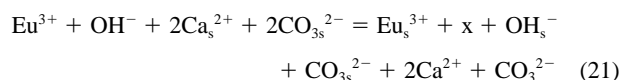
By analogy to case 1, two limiting cases can be described: one, where Eu concentration in the solid is much higher than that of thermal defects, so vacancy concentration is determined by Eu concentration in the solid: $X_x = X_{Eu}$. If at least one hydroxide ion corresponds to each Eu^{3+}, then $X_{OH} = X_{Eu}$ and we can write the equilibrium constant as:

$$K_4 = \frac{X_{Eu}^3}{X_{Ca}^2 X_{CO_3}} \frac{(Ca^{2+})^2(CO_3^{2-})}{(Eu^{3+})(OH^-)} \qquad (22)$$

where (Eu^{3+}) is proportional to X_{Eu}^3. This contradicts the experimental data as well.
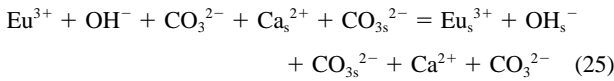
The second limiting case is where X_{Eu} is very low and defect concentration is nearly constant. In this case, the equilibrium constant looks as follows:

$$K_5 = \frac{X_{Eu}^2}{X_{Ca}^2 X_{CO_3}} \frac{(Ca^{2+})^2(CO_3^{2-})}{(Eu^{3+})(OH^-)} \qquad (23)$$

Although the power on X_{Eu} is decreased compared to the

previous equation, the presence of the hydroxide ion in the solid makes the ratio too high to correspond to the experimental data.

c) One can imagine one more possibility of compensating for the excess charge developed during substitution of Eu^{3+} for Ca^{2+}. Substitution of OH^- for CO_3^{2-} can be expressed:

$$Eu^{3+} + OH^- + CO_3^{2-} + Ca_s^{2+} + CO_{3s}^{2-} = Eu_s^{3+} + OH_s^- + CO_{3s}^{2-} + Ca^{2+} + CO_3^{2-} \quad (25)$$

from which one can write:

$$K_6 = \frac{X_{Eu}X_{OH}}{X_{Ca}} \frac{(Ca^{2+})}{(Eu^{3+})(OH^-)} \quad (26)$$

Again, because X_{Eu} has to be equal to X_{OH}, we can rewrite Eqn. 26:

$$K_6 = \frac{X_{Eu}^2}{X_{Ca}} \frac{(Ca^{2+})}{(Eu^{3+})(OH^-)} \quad (27)$$

This case does not satisfy the experimental data, because $(Eu^{3+}) \sim X_{Eu}^2$. All the more, this case holds when more than one OH^- takes part in the substitution.

3.3.3. EuNa(CO₃)²-CaCO₃ Solid Solution

Finally, we consider the coupled substitution of Eu with Na as:

$$Eu^{3+} + Na^+ + 2Ca_s^{2+} = Eu_s^{3+} + Na_s^+ + 2Ca^{2+}. \quad (28)$$
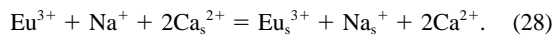
Na is one of the major components of natural ground waters so it is present to some degree in all natural calcites, either as fluid inclusions or substituted within the structure. It is also present as a trace component in synthetic commercial products. In spite of a weak tendency for alkali metals to be incorporated into calcite (Curti, 1999), such a substitution is quite promising for explanation of charge compensation in Eu substitution because of its usual presence and because its ionic radius is very similar to that of both Ca^{2+} and Eu^{3+}. In our experiments, Na was present as the cation in the CO_3 feed solutions and as $NaClO_4$, the ionic strength controller and it was also present in the experiments of Zhong and Mucci (1995), who used artificial sea water. They observed a strong positive correlation between total REE concentration and the Na^+ partition coefficient in the calcite overgrowths. Further support for the possibility of Na substitution comes from the occurrence of Ca-alkali metal-lanthanide carbonates, e.g., $KM(CO_3)_2$ (M = Nd, Gd, Dy, Ho, Yb) (Kutlu et al., 1997).

We can write an equilibrium constant for reaction 28

$$K_7 = \frac{X_{Eu}X_{Na}}{X_{Ca}^2} \frac{(Ca^{2+})^2}{(Eu^{3+})(Na^+)} \quad (29)$$

If Na content in calcite is not much higher than that of Eu, as is the case for our experiments (Table 1), then the expression for the equilibrium constant is:

$$K_7 = \frac{X_{Eu}^2}{X_{Ca}^2} \frac{(Ca^{2+})^2}{(Eu^{3+})(Na^+)} \quad (30)$$

because X_{Na} should be equal to X_{Eu}.

For the solubility products, one can write the following expressions:

$$(Eu^{3+})(Na^+)(CO_3^{2-})^2 = K^s_{EuNa(CO_3)_2} X_{EuNa(CO_3)_2} \quad (31)$$

and

$$(Ca^{2+})^2(CO_3^{2-})^2 = K^s_{Ca}{}^2 X_{Ca}^2, \quad (32)$$

where $K^S_{EuNa(CO_3)_2}$ represents the solubility product for Eu-$Na(CO_3)_2$ end member. Dividing Eqns. 32 by 31 and comparing with Eqn. 30 shows that $X_{EuNa(CO_3)_2}$ (Eqn. 31) has to be equal to X_{Eu}^2 from Eqn. 30. It is easy to see that in this case (Eu^{3+}) should be proportional to X_{Eu}^2. This model does not fit the experimental data. Indeed, no correlation can be observed between Eu and Na concentrations in calcite (Table 1). The mechanism for Na incorporation during calcite growth is probably simple occlusion or trapping in crystal defects or perhaps in fluid inclusions. The absence of a stoichiometric relationship between Na, Ca and Eu indicates that Na does not alone serve as the charge compensating species. This fits with the findings of Busenberg and Plummer (1985) from studies of calcite precipitation in Na^+ and SO_4^{2-} bearing solutions. They observed that Na^+ does not follow the Berthelot-Nernst distribution law, and the amount incorporated into the calcite structure is determined by the number of crystal defects. This agrees with the experimental results of White (1975) and Ishikawa and Ichikuni (1984) who suggested that Na^+ occupies interstitial positions in the calcite crystal. Busenberg and Plummer (1985) remarked, "The number of defects present in the crystal structure is dependent on the method of preparation, rate of crystal growth, ionic substitution, composition of the solutions, etc. The numerical values of the experimental distribution coefficients from different studies vary by a factor of 30."

4. SUMMARY

Thus, these results show that Eu from solution is strongly partitioned by calcite and uptake is independent of precipitation rate and particle size, meaning that elements with behavior similar to Eu, such as americium and curium, would be expected to be sequestered by calcite. It also suggests that the rather low concentrations of rare Earth elements (REE) in natural calcites result from low concentrations in solution rather than an inability of calcite to accommodate REE ions. From analysis of the possible mechanisms for europium incorporation into calcite and their corresponding stoichiometries, one can conclude that only models which show straight lines with slope close to 1 in a logarithmic plot of [Eu] vs. X_{Eu} are compatible with the experimental data obtained. These are the models that correspond to a solid solution with $EuOHCO_3$ or with $Eu_{2\ x}(CO_3)_3$ as the end member. Substitution of two Eu atoms and one vacancy in three Ca sites fits the stoichiometric relationships of the experimental data and the constraints of geometry in the calcite lattice. Formation of a $EuOHCO_3$-$CaCO_3$ solid solution is suspicious, because it is difficult to imagine how the incorporation of such a large unit as $EuOH^{2+}$ could result in the observed high values ($K_D \sim 800$) for the Eu partition coefficient. The evidence of Stumpf and Fanghänel (2002), that no hydroxide ion is found in the first coordination sphere of Cm(III), supports this interpretation but complete

rejection of this model requires further spectroscopic data. All other models or any combination of them give a stoichiometry $[Eu]/X_{Eu}$ higher than 1. The picture is exactly the same for comparisons with the ion activity product examined as a function of Eu molar fraction in the solid, X_{Eu}. The slope fits the experimental data only in the case of the $Eu_2{}_x(CO_3)_3$-$CaCO_3$ and $EuOHCO_3$-$CaCO_3$ solid solutions (Fig. 3).

Associate editor: D. J. Rimstidt

REFERENCES

Baker J., Waight T., and Ulfbeck D. (2002) Rapid and highly reproducible analysis of rare earth elements by multiple collector inductively coupled plasma mass spectrometry. *Geochim. Cosmochim. Acta* **66,** 3635–3646.

Busenberg E. and Plummer L. N. (1985) Kinetic and thermodynamic factors controlling the distribution of $SO_4{}^{2-}$ and Na^+ in calcites and selected aragonites. *Geochim. Cosmochim. Acta* **49,** 713–725.

Chernov A. A. (1980) Crystallization processes. In *Modern Crystallography,* vol. 3, *Crystal Formation,* pp. 7–232. Nauka.

Curti E. (1999) Coprecipitation of radionuclides with calcite: Estimation of partition coefficients based on review of laboratory investigations and geochemical data. *Appl. Geochem.* **14,** 433–445.

Davis J. A., Fuller C. C., and Cook A. D. (1987) A model for trace metal sorption processes at the calcite surface: Adsorption of Cd^{2+} and subsequent solid solution formation. *Geochim. Cosmochim. Acta* **51,** 1477–1490.

Dromgoole E. and Walter L. (1990) Iron and manganese incorporation into calcite: Effects of growth kinetics, temperature and solution chemistry. *Chem. Geol.* **81,** 311–336.

Dubinina E. O. and Lakshtanov L. Z. (1997) Separation of the oxygen isotopes while the synthesis of quartz at hydrothermal conditions (in Russian). *Proc. Rus. Min. Soc.* **76,** 11–22.

Elzinga E. J., Reeder R. J., Withers S. H., Peale R. E., Mason R. A., Beck K. M., and Hess W. P. (2002) EXAFS study of rare-earth element coordination in calcite. *Geochim. Cosmochim. Acta* **66,** 2875–2885.

Henderson L. M. and Kracek F. C. (1927) The fractional precipitation of barium and radium chromates. *J. Am. Chem. Soc.* **49,** 739–749.

Hummel W., Berner U., Curti E., Pearson F. J. Jr., Thoenen T. (2002) Nagra/PSI chemical thermodynamic data base. 01/01. Technical Report NTB 02-16. Nagra.

Ishikawa M. and Ichikuni M. (1984) Uptake of sodium and potassium by calcite. *Chem. Geol.* **42,** 137–146.

Kelting H. and Witt H. (1949) Ueber KCl-Kristalle mit Zusatzen von Erdalkalichloriden. *Z. Phyzik.* **126,** 697–710.

Kutlu I., Kalz H. J., Wartchow R., Ehrhardt H., Seidel H., and Meyer G. (1997) Kalium-lanthanoid-carbonate, $KM(CO_3)_2$ (M = Nd, Gd, Dy, Ho, Yb). *Z. Anorg. Allg. Chem.* **623,** 1753–1758.

Lippmann F. (1980) Phase diagrams depicting aqueous solubility of binary mineral systems. *Neues Jahrb. Miner. Abh.* **139,** 1–25.

Lorens R. (1981) Sr, Cd, Mn, and Co distribution coefficients in calcite as a function of calcite precipitation rate. *Geochim. Cosmochim. Acta* **45,** 553–561.

McIntire W. L. (1963) Trace elements partition coefficients—A review of thery and application to geology. *Geochim. Cosmochim. Acta* **27,** 1209–1264.

Meece D. E. and Benninger L. K. (1993) The coprecipitation of Pu and other radionuclides with $CaCO_3$. *Geochim. Cosmochim. Acta* **57,** 1447–1458.

Mucci A. and Morse J. W. (1983) The incorporation of Mg^{2+} and Sr^{2+} into calcite overgrowths: Influences of growth rate and solution composition. *Geochim. Cosmochim. Acta* **47,** 217–233.

Palmer M. R. (1985) Rare earth elements in foraminifera tests. *Earth Planet. Sci. Lett.* **73,** 285–298.

Paquette J. and Reeder R. J. (1995) Relationship between surface structure, growth mechanism, and trace element incorporation in calcite. *Geochim. Cosmochim. Acta* **59,** 735–749.

Parekh P. P., Möller P., Dukski P., and Bausch W. M. (1977) Distribution of trace elements between carbonate and non-carbonate phases of limestone. *Earth Planet. Sci. Lett.* **34,** 39–50.

Parkhurst D. L. and Appelo C. A. J. (1999) User's guide to PHREEQC (version 2)—A computer program for speciation, bath-reaction, one-dimensional transport and inverse geochemical calculations. Water-Resources Investigations Report 99-4259. U.S. Geological Survey.

Parkman R. H., Charnock J. M., Livens F. R., and Vaughan D. J. (1998) A study of the interaction of strontium ions in aqueous solution with the surfaces of calcite and kaolinite. *Geochim. Cosmochim. Acta* **62,** 1481–1492.

Piriou B., Fedoroff M., Jeanjean J., and Bercis L. (1997) Characterization of the sorption of europium (III) on calcite by site-selective and time-resolved luminescence spectroscopy. *J. Colloid Interface Sci.* **194,** 440–447.

Rimstidt J. D., Balog A., and Webb J. (1998) Distribution of trace elements between carbonate minerals and aqueous solutions. *Geochim. Cosmochim. Acta* **62,** 1851–1863.

Stipp S. L. and Hochella M. F. (1991) Structure and bonding environments at the calcite surface as observed with X-ray spectroscopy (XPS) and low-energy electron diffraction (LEED). *Geochim. Cosmochim. Acta* **55,** 1723–1736.

Stipp S. L. S., Lakshtanov L. Z., Jensen J. T., and Baker J. A. (2003) Eu^{3+} uptake by calcite: Preliminary results from coprecipitation experiments and observations with surface-sensitive techniques. *J. Contam. Hydrol.* **61,** 33–43.

Stumpf T. and Fanghänel T. (2002) A time-resolved laser fluorescence spectroscopy (TRLFS) study of the interaction of trivalent actinides (Cm(III)) with calcite. *J. Colloid Interface Sci.* **249,** 119–122.

Terakado Y. and Masuda A. (1988) The coprecipitation of rare-earth elements with calcite and aragonite. *Chem. Geol.* **69,** 103–110.

Tesoriero A. and Pankow J. (1996) Solid solution partitioning of Sr^{2+}, Ba^{2+}, and Cd^{2+} to calcite. *Geochim. Cosmochim. Acta* **60,** 1053–1063.

Urusov V. S., Tauson V. L., and Akimov V. V. (1997) *Geochemistry of Solids.* GEOS.

Urusov V. S. and Dudnikova V. B. (1998) The trace-component trapping effect: Experimental evidence, theoretical interpretation, and geochemical applications. *Geochim. Cosmochim. Acta* **62,** 1233–1240.

Wang Y. and Xu H. (2001) Prediction of trace metal partitioning between minerals and aqueous solutions: A linear free energy correlation approach. *Geochim. Cosmochim. Acta* **65,** 1529–1543.

Watson E. B. and Liang Y. (1995) A simple model for vector zoning in slowly grown crystals: Implications for growth rate and lattice diffusion, with emphasis on accessory minerals in crustal rocks. *Am. Miner.* **80,** 1179–1187.

White A. F. (1975) Sodium and potassium coprecipitation in calcium carbonate. PhD. Dissertation. Northwestern University, Evanston, Illinois.

Zhong S. and Mucci A. (1995) Partitioning of rare earth elements (REEs) between calcite and seawater solutions at 25°C. *Geochim. Cosmochim. Acta* **59,** 443–453.